ORIGINAL ARTICLE

Evaluation of the Changes in the Shape and Location of the Prostate and Pelvic Organs Due to Bladder Filling and Rectal Distension

M Lotfi [1], MH Bagheri[1], MA Mosleh-Shirazi [2], R Faghihi [3], M Baradaran-Ghahfarokhi [4*]

[1] Medical Imaging Research Center and Radiology Department, Shiraz University of Medical Sciences, Shiraz, IR Iran

[2] Center for Research in Medical Physics and Engineering and Radiotherapy Department , Namazi Hospital, Shiraz University of Medical Sciences, Shiraz, IR Iran

[3] Radiation Research Center and Mechanical Engineering Department, School of Engineering, Shiraz University, Shiraz, IR Iran

[4] Medical Physics and Medical Engineering Department, School of Medicine, Isfahan University of Medical Sciences, Isfahan, IR Iran

Abstract

Background: Prostate brachytherapy has become an increasingly popular treatment for localized prostate cancer. A steep dose gradient between the prostate and organs at risk (rectum and bladder) is ideal in this treatment modality, so prostate displacement and deformation due to bladder filling and rectal distension play an important role in critical organs post-implant dose. The purpose of this study was to evaluate the interrelationship between normal rectal distension, bladder filling, and their movements. The study also aimed to quantify total prostate displacement and deformation due to physiologic organ filling measured by using magnetic resonance imaging (MRI) based shifts and estimate the precision with which the shifts were made in supine and left decubitus positions.

Patients and Methods: 3 patients who were referred for transrectal prostatic biopsy (Shahid Faghihi hospital, Shiraz, Iran) with different prostate sizes were selected for this study. A 1.5-Tesla MRI system (Avanto, Siemens, Germany) and an ultrasound system (Logiq 500, GE medical systems, USA) were used to collect images of the patients' prostates at different stages of bladder and rectum fullness.

Results: The mean displacement of the prostate after bladder filling in the supine and left decubitus positions along the anterior-posterior (AP) axis was posterior by 3.5 mm (range = 0.7 mm to 6.3 mm) and along the superior-inferior (SI) axis was inferior by 3.4 mm (range = 1.4 mm to 5 mm). Prostate displacement in the left-right (LR) axis was negligible. The mean prostate displacement after rectal distension was anterior by 7.1 mm in the supine position, 5.1 mm anterior in the left decubitus position, and along the SI axis was inferior by 2.9 mm in the supine and left decubitus positions. The maximum prostate deformation due to rectal distension and bladder filling in the supine position was as large as 3.2 mm, 1.9 mm, and 1.2 mm in the AP, SI, and LR directions, respectively. While in the left decubitus position, maximum prostate deformation was 2.6 mm, 1.2 mm, and 1.3 mm in the AP, LR, and SI directions, respectively.

Conclusions: It is probably important to evaluate the influence of the changes in the shape and location of the prostate due to bladder filling, rectal distension, and patient position in post-implant brachytherapy dosimetry. Using images of patients in the left decubitus position with a full bladder and distended rectum is suggested in planning for treatment.

Keywords: Prostate displacement; Deformation; Magnetic Resonance Imaging; Ultrasonography

Introduction

In developed countries, prostate cancer is the second-most frequently diagnosed type of cancer and the third-most common cause of death from cancer in men (1).

* *Corresponding author at:* Milad Baradaran-Ghahfarokhi, Medical Physics and Medical Engineering Department Isfahan University of Medical Sciences, Isfahan, IR Iran. Tel: +98-9133155377, Fax: +98-3116688597, *e-mail:*milad_bgh@yahoo.com

Today prostate brachytherapy has become an increasingly popular treatment for localized prostate cancer (2). In prostate brachytherapy, a steep dose gradient between prostate and organs at risk (rectum and bladder) is ideal, so prostate displacement and deformation may be critical to the total dose delivered to each organ (3-5). However, it is known that the anatomical position of the prostate gland can be affected by the physiological movements of the surrounding pelvic organs such as

the rectum and bladder. A consequence of this motion in brachytherapy may be an increased radiation dose to surrounding normal tissues. Previous authors have demonstrated that movements of the prostate relative to the bony pelvis were associated with differential filling of the bladder and bowel (6). Using Computed Tomography (CT) imaging, Deurloo *et al.* found that the prostate behaved as a rigid body (7), whereas using cine magnetic resonance imaging (cine-MRI), Ghilezan *et al.* found that it deformed in the anteroposterior (AP) direction (8). Most studies assessing prostate movement have imaged the prostate gland by repeated CT scans over the course of radiotherapy (9, 10). Although these assessments have been repeated serially, all of these studies have evaluated prostate position in a very limited time frame. Other direct imaging techniques such as seed implants and ultrasound imaging, (11-13) kilovoltage (kV), cone beam computed tomography (CBCT), (14, 15) and CT on rails (16) have been used to study prostate displacement. Seed implants method is an invasive method. Additionally, the Fiducial Markers (FMs) might migrate within the gland. Shirato *et al.* observed a significant in-migration of prostatic FMs for patients treated without hormones, and some authors have observed no significant in-migration of prostatic FMs (17-19). However, other authors did not describe a time dependence of intermarker distances (20, 21). Ultrasonography (US) is simple, quick, noninvasive, painless, and repeatable. Its accuracy has been proven but is less accurate than other methods and completely depends on the radiologist's skill. Also, pressure from the US probe causes organs to move. When images of the prostate are obtained with an endorectal ultrasound probe or magnetic resonance imaging (MRI) coil, it is apparent that the prostate can deform. The CT method has low contrast in delineating soft tissue with slack of radiation protection. Modern imaging systems such as Megavoltage (MV) portal imaging devices inherently have lower contrast than kV images because of a greater percentage of Compton interaction (22). This may blur prostatic borders, especially at the bladder interface. MRI is a good method to assess the prostate and its neighboring organs. MRI enables direct visualization

of soft-tissue targets and organs at risk at the expense of time and cost, as opposed to US and CT. This study had two objectives. The first was to evaluate the interrelationship between normal rectal distension and bladder filling and their movements. The second was to quantify total prostate displacement and deformation due to physiologic organs filling measured by MRI-based shifts and estimate the precision with which the shifts were made in the supine and left decubitus positions. It is our assumption that breathing doesn't cause obvious prostate displacement (23). We also used US imaging in addition to MRI. To the best of our knowledge, this the first study of prostate displacement and deformation due to rectal distension and bladder filling simultaneously in two different positions (supine and left decubitus). Knowledge of these displacements is clinically relevant because planning a brachytherapy is limited to the supine and lithotomy positions and neglects the stages of organ filling and other patient-related daily positions (such as decubitus) encountered during the postimplant prostate irradiation period.

Patients and Methods

The study protocol was approved by the Medical Imaging Research Center at the Shiraz University of Medical Sciences. Patients were eligible if they had prostatic problems and gave written, informed consent to the study and underwent diagnostic pelvic MRI and transabdominal US imaging for staging purposes. *Table1* shows the patients' characteristics.

MR Imaging

A 1.5-Tesla MRI system (Avanto, Siemens, Germany) was used to collect sequential axial and sagittal images of patients' prostates with different sizes. Routine T1- and T2-weighted sequences with a pelvic coil were used for the MRI. A contrast agent was not administered. For each patient, four sets of images in three stages were obtained. In an axial T1- weighted (T1-w) turbo factor (spin echo) sequence, the field of view (FOV) was 36 cm, the matrix was 512 × 512, time repetition (24)/time echo (TE) was 718/10 ms, and slice thickness (ST) was 3 mm. In the T2-weighted (T2-w) turbo factor (spin echo) sequence, the FOV was 36 cm, the matrix was 512 × 512, TR/TE was 3200/73 ms, and ST was 3 mm. In a sagittal T1-weighted (T1-w) turbo factor spin echo sequence, the FOV was 25

Table 1. Patient characteristics

Characteristic	Mean (range)
Age, y	54 (26-67)
interval between biopsy and MRI [a], w	4 (3-5)
maximal AP [b] dimensions of the patients at the level of the prostate, mm	44.6 (23.3-55.9)
Maximal lateral dimensions of the patients at the level of the prostate, mm	47.2 (24.4-59.1)
prostate-specific antigen level, ng/mL	10 (9.8-10.2)
Prostate size, mL	54.6 (32-71)
Gleason biopsy score	5 (4-6)

[a] MRI: magnetic resonance imaging
[b] AP: Anterbor-posterior

Table 2. Imaging study stages

Study stages	Rectum	Bladder
I	D [a]	F [b]
II	E [c]	E
III	E	F

[a] D = Distended
[b] F = Full
[c] E = Empty

Table 3. Bladder volume and surface area in full and empty bladder

	Stage [a]	Volume, cm³	Surface area [b], cm²	
			Supine	Left decubitus
P1 [c]	F [d]	383	228.9	239.9
	E [e]	160	68.8	76.8
P2	F	256.8	108.8	150.7
	E	94.8	41.1	59.4
P3	F	180	105.1	115.2
	E	26	16.1	19.8
Mean ± SD	F	266.6 ± 102.5	147.6 ± 70.4	168.6 ± 64.2
	E	93.6 ± 67	42 ± 26.4	52 ± 29.2

[a] Patients were instructed to drink 1 liter of water before Stage III.
[b] Surface area is the product of maximum bidimensional diameter at the level of the prostate.
[c] P1 refers to the first patient.
[d] E: Empty
[e] F: Full

cm, TR/TE was 350/12 ms, and ST was 4 mm with 0 mm gap. A sagittal T2 spin echo sequence was acquired to accurately position the prostate apex on the cranio–caudal axis (24, 25). For the imaging stages, first scans were done of the patients' full bladders and rectums 8 hours after their fibrous meal and were instructed not to empty their bladders or rectums before planning the first MRI. Then, patients were imaged in the supine and left decubitus positions on a flat tabletop and set up using a set of triangulation lasers. Next, they were instructed to empty their bowels and bladder as much as possible and were imaged as described above. Antiperistaltic medications were not employed because purge medications affect normal physiological movements of the rectum. Furthermore, they were instructed to drink 1 L of fluid 1 h before planning the third MRI. This bladder and bowel regimen was intended to ensure that they were comfortably full or empty at the time of imaging. *Table 2* shows the imaging study stages. The images from all sequences were used to evaluate the interrelationship between rectal distension and bladder filling and rectal, bladder

movement, and the effect of their movement on prostate gland shape and position. The MR images were initially acquired using a separate program and then imported into Advantage Workstation version 4.3 (GE medical systems) software for organ position measurements. An expert radiologist in prostate MRI interpretation reviewed all imaging sets. He contoured the prostate and its neighboring organs for each patient (*Figure 1*). For each image, the rectum, bladder, and prostate gland were outlined on the second stage images (baseline), and organ movements in the first and third stage were measured relative to the baseline (second stage). The images were analyzed for the magnitude of rectal distension and bladder filling, prostate deformation, displacement, and rotation relative to the baseline prostate outline.

Prostate and bladder volumes

The volumes were calculated by manually determining the prostate outline on every axial T1-weighted MRI slices. The reader drew a freehand contour around the prostate

Table 4. Rectal surface area in distended and empty rectum

	Stage	Surface area, mm²	
		Supine	Left decubitus
P1	D [a]	4481.2	3404.8
	E [b]	1466.9	1467.0
P2	D	2730.0	2857.8
	E	450.5	491.6
P3	D	513.8	716.0
	E	262.7	278.5
Mean ± SD	D	2575.0 ± 1988.2	2326.2 ± 1421.0
	E	726.7 ± 647.9	745.7 ± 633.7

[a] D: Distended
[b] E: Empty

Table 5. Bladder motion in the superior inferior direction

	Stage	SI [a] diameter, mm	
		Supine	Left decubitus
P1	F [b]	182.4	190.1
	E [c]	29.3	34.1
P2	F	69.6	80.9
	E	6.1	10.3
P3	F	35.4	79.7
	E	6.0	10.2
Mean ± SD	F	95.8 ± 76.9	116.9 ± 63.4
	E	13.8 ± 13.4	18.2 ± 13.8

[a] SI: Superior inferior
[b] F: Full
[c] E: Empty

Table 6. Rectal motion in the anterior posterior direction

	Stage	AP [a] diameter, mm	
		Supine	**Left decubitus**
P1	F [b]	44.8	47.5
	E [c]	12.7	16.1
P2	F	34.9	40.2
	E	11.7	16.0
P3	F	10.3	26.3
	E	9.8	10.2
Mean ± SD	F	30 ± 17.8	38.0 ± 10.7
	E	11.4 ± 1.5	14.1 ± 3.4

[a] AP: Anterior posterior
[b] F: Full
[c] E: Empty

on each imaging slice on the Advantage Workstation. For each slice, the number of pixels within the contour was automatically established, and the prostate and bladder volumes were calculated with the known in-plane resolution and slice thickness.

Rectal distension and bladder filling

Rectal distension and bladder filling were measured by the product of the maximum bidimensional axial and sagittal diameters at the level of the prostate. The maximum bidimensional diameter product was calculated as the product of the longest and widest diameter of the rectum and bladder taken perpendicularly (*Figure 2*).

Organ motion

Organ motion was assessed by the maximum motion measurement in all three directions (AP, LR, SI) in the axial and sagittal images relative to baseline (second stage). For example, bladder motion in the lateral direction was obtained from the maximum membrane displacement in the LR axis and in the axial image relative to fix bony pelvic.

Prostate deformation

We assessed the changes of the prostate size in three directions relative to the Stage II images. The largest medial AP and LR diameters were measured in the axial plane, and the largest SI diameter was assessed in the sagittal plane (*Figure 3*).

Prostate displacement

Prostate displacements from the baseline position in the AP, LR, and SI directions occurring as a result of rectal distension and bladder filling were measured relative to the pelvic bony structure in the sagittal and axial images. (*Figures 4 and 5*) show extreme examples of motion from an axial and sagittal scan of initial patient anatomy in both positions. Three different frames were shown for each plane. The initial frames show the first image and one later image in the series. The third frame shows the differences in the images by superimposing the first two.

Intraobserver error was estimated by performing the same measurements on a patient two times by single observer. The same plane was found each time from the pixel coordinates. The position of the edge of the prostate along the plane defined by a particular x or y pixel value was assessed two times for the same image.

US Imaging

US imaging was conducted before each MRI stage. This made us confident of organ fullness. Suprapubic images were acquired with an ultrasound system (Logiq 500, GE medical systems, USA) with patients in the MRI position by an expert radiologist. The US device was equipped with a digital display screen and a handheld transabdominal scanning head. Ultrasound localization of the prostate and neighboring organs was performed immediately before MRI to decrease the effect of organ filling on the measurement's accuracy.

Prostate and bladder volumes

Prostate and bladder volumes were measured by an expert radiologist. The scanning head was positioned at the midline above the pubic symphysis, and the volume was calculated manually by the radiologist. Longitudi-

Table 7. Prostate displacement after bladder filling

	Supine, mm			Left decubitus, mm		
	AP [a]	**SI [b]**	**LR [c]**	**AP [a]**	**SI [b]**	**LR [c]**
P1	- 5.3 [d]	- 4.0	1.6	- 6.3	- 5.0	4.7
P2	- 2.4	- 3.6	0.4	- 4.0	- 4.1	4.1
P3	- 0.7	- 2.0	0.4	- 2.0	- 1.4	0.8
Mean ± SD	- 2.8 ± 2.3	- 3.2 ± 1.1	0.8 ± 0.7	- 4.1 ± 2.2	- 3.5 ± 1.9	3.2 ± 2.1

[a] AP: Anterior posterior
[b] SI: Superior inferior
[c] LR: Left right
[d] It is our assumption that anterior, superior, left motion is positive, so negative values refer to prostate movement to the posterior, inferior, and righ.

Table 8. Prostate displacement and deformation after bladder filling and rectal distension

	Supine, mm			Left decubitus, mm		
	AP [a]	SI [b]	LR [c]	AP [a]	SI [b]	LR [c]
P1	6.5	- 4.4	1.1	7.3	- 2.9	1.7
P2	6.5	- 3.5	1.0	4.1	- 2.6	1.4
P3	8.3	- 1.1	0.9	3.9	- 2.0	1.1
Mean ± SD	7.1 ± 1.0	- 3.0 ± 1.7	1.0 ± 0.1	5.1 ± 1.9	- 2.5 ± 0.5	1.4 ± 0.3

[a] AP: Anterior posterior
[b] SI: Superior inferior
[c] LR: Left right

nal and transverse scans that give the greatest diameter were obtained with the transducer positioned above the symphysis pubis. The width (W), length (L), and cranio-caudal diameter (height [H]) in the sagittal plane were recorded (*Figure 6*). We used the formula described by the radiologist to calculate the bladder and prostate volume.

$$V = H(W \times L) \times 0.52$$

Trained US and MRI measurements were performed two times for each organ. For the statistical analysis, the mean of measurements were denoted as Vbl-US, Vpr-US, and Vbl-MRI,Vpr-MRI. To evaluate the relationships between Vbl-US, Vpr-US, and Vbl-MRI,Vpr-MRI, a Wilcoxon test was performed. Data were analyzed using SPSS software version 16.0. $P \leq 0.05$ was considered statistically significant.
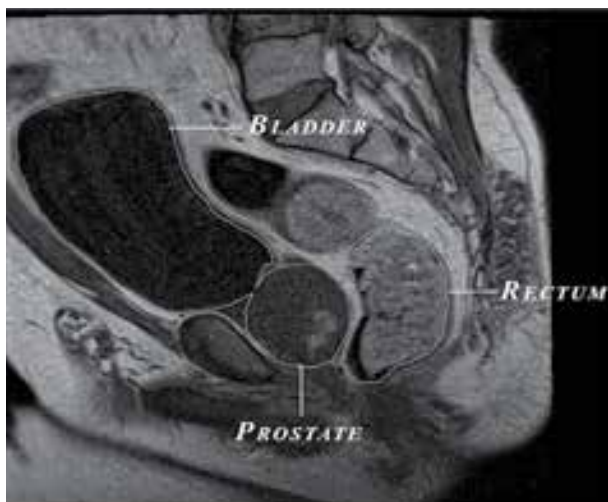
Results

Prostate and bladder volumes

Tables 3 and *4* illustrate bladder and rectal volumes and surface areas in the supine and left decubitus positions.

Rectal distension and bladder filling

Figure 1. Organs contouring in the stage I

As discussed above, Figures 4 and 5 show an example of organ motion due to changes in filling of the bladder and rectum. The maximum bidimensional area of the distended rectum was 68 × 65.9 mm, whereas it was 43.4 × 33.8 mm for the empty rectum.

Organ motion

Bladder filling as well as rectal distension resulted in prostate displacements in all directions. Filling of the bladder resulted in bladder displacement, especially in the anterior and cranial directions. Emptying the rectum but maintaining a full bladder resulted in an overall posterior movement of the bladder. The ranges for bladder motion in each of the directions were large, indicating a considerable variation in organ motion in each of the patients. Comparing MR images in Stages I and II, distension of the rectum resulted in rectal motion in the AP direction. In the left decubitus position, bladder tended to move in the LR direction more than rectum.

Prostate deformation

The maximum prostate deformation in the supine position was as large as 3.2 mm, 1.9 mm, and 1.2 mm in the AP, SI, and LR directions, respectively. Maximum deformation in the left decubitus position was 2.6 mm, 1.2 mm, and 1.3 mm in the AP, SI, and LR directions, respectively.

Prostate displacement

The maximum and mean displacement of the prostate gland after bladder filling in the supine and left decubitus positions along the AP axis was posterior by 6.3 mm and 3.5 mm, respectively (range = posterior displacement of 0.7 mm to 6.3 mm) and along the SI axis was inferior by 5 mm and 3.4 mm, respectively (range = inferior displacement 1.4 mm to 5 mm). In the supine position prostate displacement in the LR axis was negligible. The maximum and mean prostate displacements and deformations after rectal distension were anterior by 8.3 mm and 7.1 mm, respectively (range = anterior displacement of 6.5 mm to 8.3 mm) in the supine position, 7.3 mm and 5.1 mm anterior in the left decubitus position, and along the SI axis was inferior by up to 4.4 mm and 2.9 mm in

Figure 2. Maximum bidimensional diameters of the organs in Stages III and I, (A) bladder sagittal, (B) rectum axial
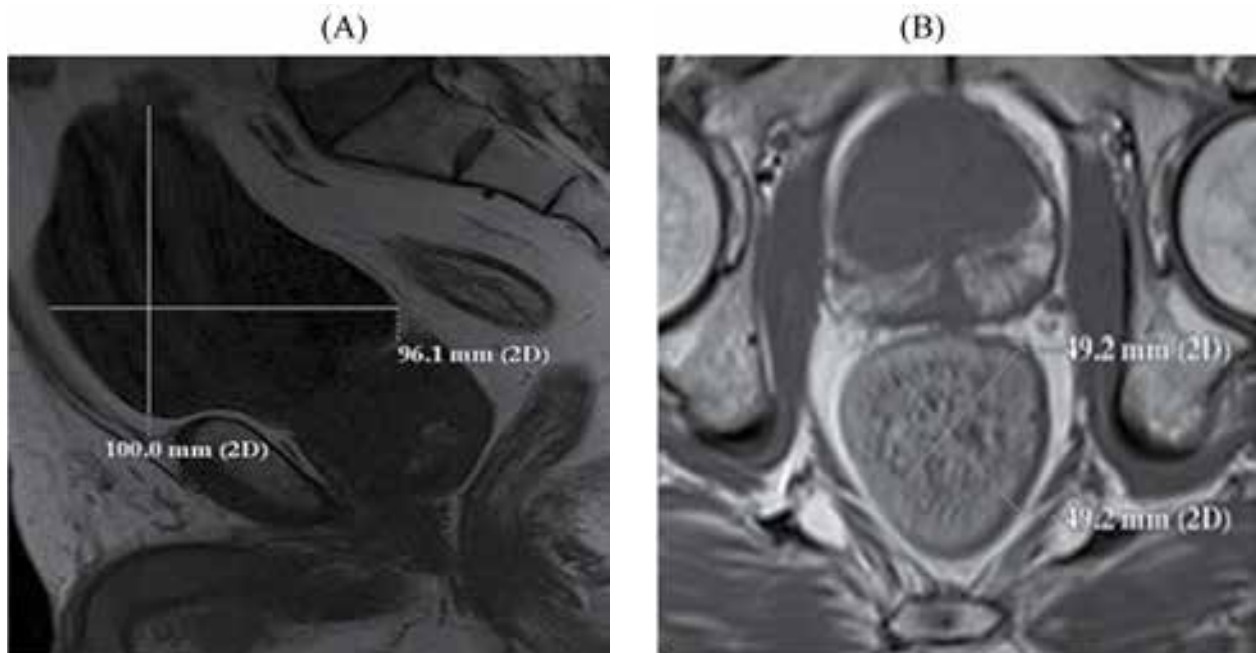
the supine and left decubitus positions (range = inferior displacement 1.1 mm to 4.4 mm). Prostate displacement due to bladder filling in the LR direction was negligible. Large rectal movements were more likely to result in more than 7.6 mm of prostatic displacement and 3.2 mm of its deformation.

Large systematic rotations of the prostate about the LR axis have been observed (SD = 1°) Maximum and median rotations of the prostate were 5° and 4.6° after distension of the rectum (range = 4° to 5°) in the supine position and 4° and 3.6° (range = 3° to 4°) in the left decubitus position. Bladder filling causes negligible prostate rotation.

In the statistical analysis, based on a total of 18 US measurements, a strong relationship between V_{bl-US}, V_{pr-US}, and V_{bl-MRI}, V_{pr-MRI} was found ($P = 0.260$), indicating a high accuracy of the US measures.

Discussion

In prostate brachytherapy, treatment plans were performed in the supine and lithotomy positions. We observed that moving to the left decubitus position caused significant changes in the shape and location of the pelvic organs. This may increase the hazard of the radiation to the normal surrounding organs in this treatment modality. Also in brachytherapy, US is used for the seed implant, but its accuracy is completely dependent on the radiologist's skill, and its FOV is restricted. Compared to CT

Figure 3. Prostate deformation in the supine position, Stage I (A), relative to baseline, Stage II (B).
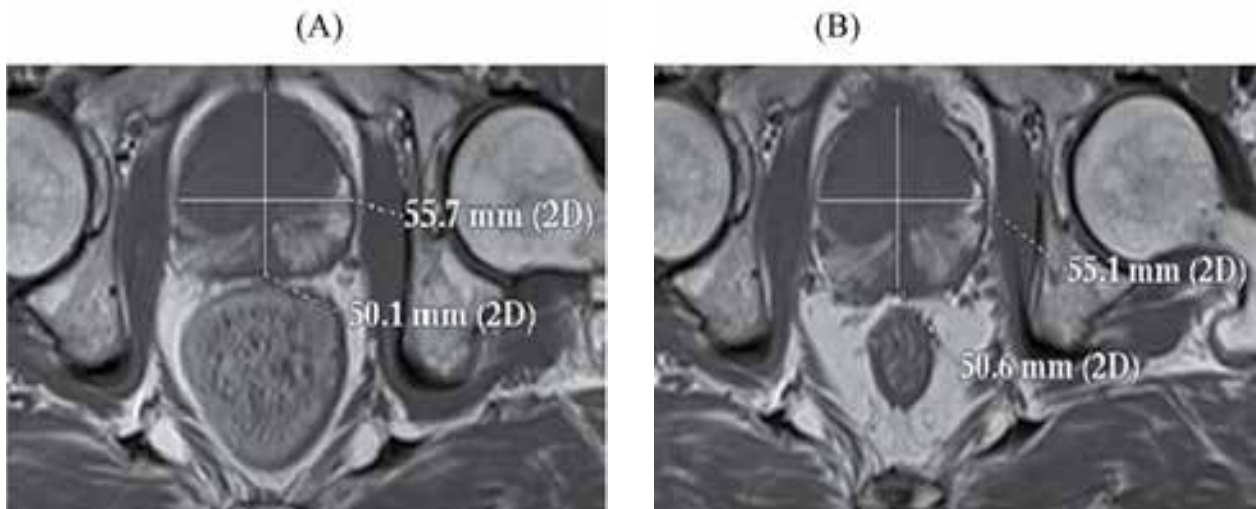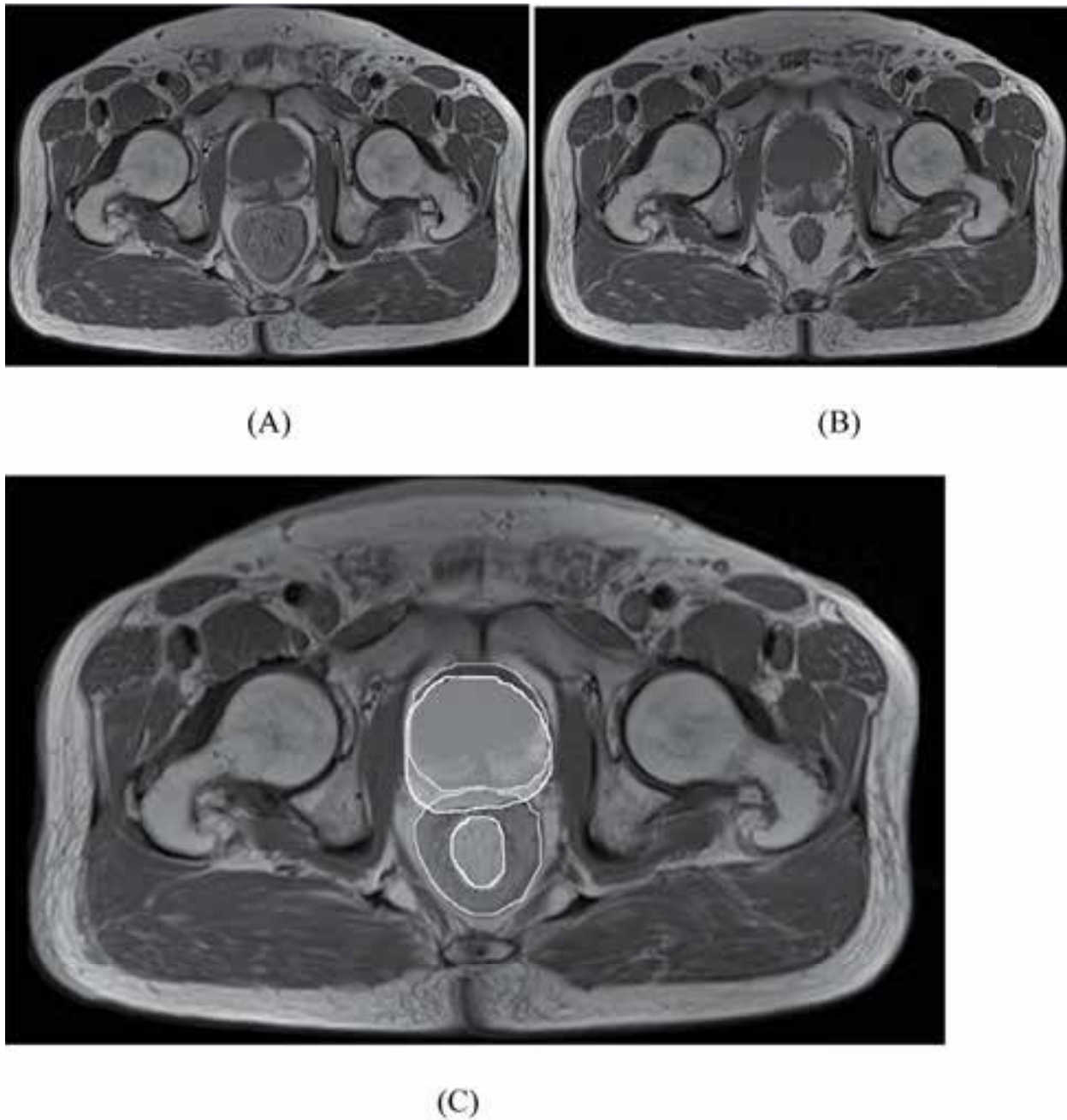
Figure 4. Axial image fusion of the patient's anatomy in the supine position, Stage I (A), Stage II (B) and fused image (C)

(A)

(B)

(C)

and US imaging, MRI can provide more reproducible delineations of the prostate. T1-weighted images have been shown to have excellent properties for soft-tissue imaging of the prostate and its neighboring organs (bladder and rectum). MRI also provides good delineation of the organs contact area. In our study, the organ volumes obtained on the MR image sets were highly reproducible. The most detailed previous study on prostate and seminal vesicle deformation was by Deurloo *et al.*(7) who quantified the shape variations of the prostate and semi-

nal vesicles using repeated CT scans. It could be argued that the prostate deformation observed in this study was due to rectal distension; however, countering error could trace it. The maximum error of the contouring was less than 1 mm, which was assessed by a recontouring process. Previous authors have demonstrated that movements of the prostate relative to the bony pelvis were related to differential filling of the bladder and bowel (6). In addition, prostate deformation under the influence of changes in physiologic rectal filling was observed in

Figure 5. Sagittal image fusion of the patient's anatomy in the supine position, Stage I (A), Stage II (B) and fused image (C)
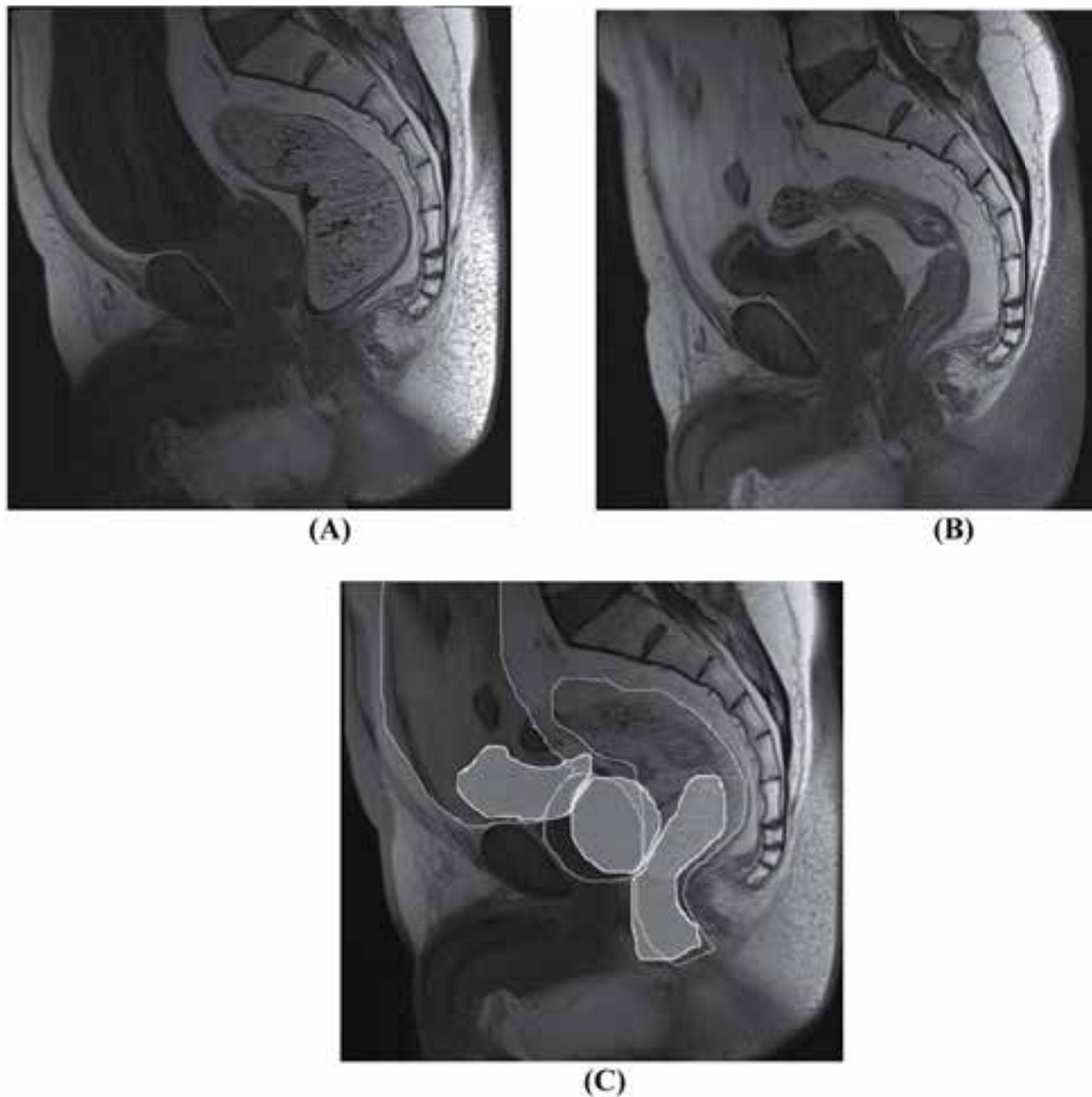
a study using cine-MRI (8). Our results showed that prostate deformation was significantly related to physiologic rectal filling. There were significant differences in the magnitude of the prostate displacement due to bladder filling or rectal distension. For larger displacements, the base of the prostate has a larger amplitude of motion than the apex, presumably because the levator muscles anchor the prostate at the apex. These results were consistent with the observations of previous studies (26) (27) However, most of the prostate displacements were in the superior and anterior directions. There was a statistically significant difference between the motions that

occurred with the empty rectum compared to the full rectum. For larger rectal motions, the prostate appeared to be both compressed in the AP direction and forced in the superior direction. Our results were generally consistent with the results of Padhani *et al.*(27) who found a correlation between the degree of rectal distension and prostate displacement. Because we had different sized patient populations at the level of the pelvis, our results provide general data about prostate displacement, deformation, and rotation. In addition, there were significant differences between the motions we measured in the AP and SI directions on both axial and sagittal scans

Figure 6. Bladder volume calculation from the longitudinal and transverse scans
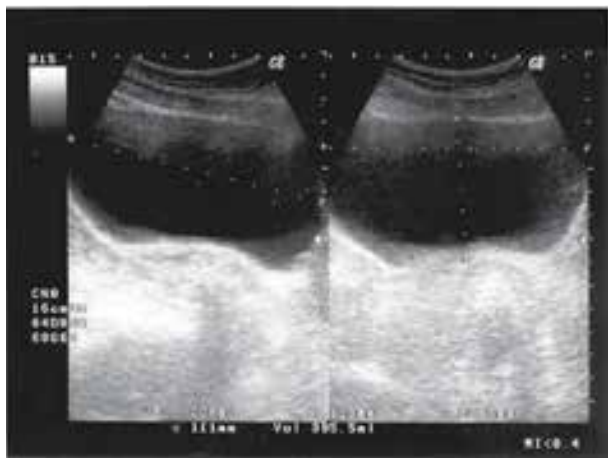
and the measurements found by Padhani *et al.* The reasons for these differences may be due to differences in organ sizes, patient diet, and time since last meal before imaging. Another possible reason for the differences may have to do with our approaches to measure motion. Padhani et al. measured the center of mass, and we measured the border of the prostate. Nevertheless, the measurement methods probably only accounted for a small part of the differences. We noted that there were no significant displacements of bony landmarks (<1 mm) during the stages of scans. We did not correct for these small motions because, during brachytherapy, it is the motion of the prostate relative to the neighboring organs and not the bony anatomy that affects the dose received by the organs (28). After rectal distension, there were no differences in the magnitude of mean prostate movement when we compared patients with early prostate tumors to those with no tumors. Bladder filling, rectal distension, and patient position cause significant changes in the shape and location of the pelvis organs. It is important to evaluate the influence of the changes in the shape and location of the prostate due to bladder filling, rectal distension, and patient posture in postimplant brachytherapy dosimetry. Using images of the patient in the left decubitus position with a full bladder and distended rectum are suggested in planning for treatment.

Financial support

Conflict of Interest

None declared.

Acknowledgement

References

1. Damber JE, Aus G. Prostate cancer. *Lancet*. 2008;**371**(9625):1710-21.
2. Machtens S, Baumann R, Hagemann J, Warszawski A, Meyer A, Karstens JH, et al. Long-term results of interstitial brachytherapy (LDR-Brachytherapy) in the treatment of patients with prostate cancer. *World J Urol*. 2006;**24**(3):289-95.
3. Pollack A, Zagars GK, Starkschall G, Antolak JA, Lee JJ, Huang E, et al. Prostate cancer radiation dose response: results of the M. D. Anderson phase III randomized trial. *Int J Radiat Oncol Biol Phys*. 2002;**53**(5):1097-105.
4. Storey MR, Pollack A, Zagars G, Smith L, Antolak J, Rosen I. Complications from radiotherapy dose escalation in prostate cancer: preliminary results of a randomized trial. *Int J Radiat Oncol Biol Phys*. 2000;**48**(3):635-42.
5. Ten Haken RK, Forman JD, Heimburger DK, Gerhardsson A, McShan DL, Perez-Tamayo C, et al. Treatment planning issues related to prostate movement in response to differential filling of the rectum and bladder. *Int J Radiat Oncol Biol Phys*. 1991;**20**(6):1317-24.
6. van Herk M, Bruce A, Kroes AP, Shouman T, Touw A, Lebesque JV. Quantification of organ motion during conformal radiotherapy of the prostate by three dimensional image registration. *Int J Radiat Oncol Biol Phys*. 1995;**33**(5):1311-20.
7. Deurloo KE, Steenbakkers RJ, Zijp LJ, de Bois JA, Nowak PJ, Rasch CR, et al. Quantification of shape variation of prostate and seminal vesicles during external beam radiotherapy. *Int J Radiat Oncol Biol Phys*. 2005;**61**(1):228-38.
8. Ghilezan MJ, Jaffray DA, Siewerdsen JH, Van Herk M, Shetty A, Sharpe MB, et al. Prostate gland motion assessed with cine-magnetic resonance imaging (cine-MRI). *Int J Radiat Oncol Biol Phys*. 2005;**62**(2):406-17.
9. Beard CJ, Kijewski P, Bussiere M, Gelman R, Gladstone D, Shaffer K, et al. Analysis of prostate and seminal vesicle motion: implications for treatment planning. *Int J Radiat Oncol Biol Phys*. 1996;**34**(2):451-8.
10. Roach M, 3rd, Faillace-Akazawa P, Malfatti C. Prostate volumes and organ movement defined by serial computerized tomographic scans during three-dimensional conformal radiotherapy. *Radiat Oncol Investig*. 1997;**5**(4):187-94.
11. Simforoosh N, Dadkhah F, Hosseini SY, Asgari MA, Nasseri A, Safarinejad MR. Accuracy of residual urine measurement in men: comparison between real-time ultrasonography and catheterization. *J Urol*. 1997;**158**(1):59-61.
12. Bih LI, Ho CC, Tsai SJ, Lai YC, Chow W. Bladder shape impact on the accuracy of ultrasonic estimation of bladder volume. *Arch Phys Med Rehabil*. 1998;**79**(12):1553-6.
13. Scarbrough TJ, Golden NM, Ting JY, Fuller CD, Wong A, Kupelian PA, et al. Comparison of ultrasound and implanted seed marker prostate localization methods: Implications for image-guided radiotherapy. *Int J Radiat Oncol Biol Phys*. 2006;**65**(2):378-87.
14. Smitsmans MH, Wolthaus JW, Artignan X, de Bois J, Jaffray DA, Lebesque JV, et al. Automatic localization of the prostate for on-line or off-line image-guided radiotherapy. *Int J Radiat Oncol Biol Phys*. 2004;**60**(2):623-35.
15. Letourneau D, Martinez AA, Lockman D, Yan D, Vargas C, Ivaldi G, et al. Assessment of residual error for online cone-beam CT-guided treatment of prostate cancer patients. *Int J Radiat Oncol Biol Phys*. 2005;**62**(4):1239-46.
16. Dong L, Crevoisier Rd, Bonnen M ea. Evaluation of an ultrasound-based prostate target localization technique with an in-room CT-on-rails [abstract]. *Int J Radiat Oncol Biol Phys*. 2004;**60**:332-3.
17. Litzenberg D, Dawson LA, Sandler H, Sanda MG, McShan DL, Ten Haken RK, et al. Daily prostate targeting using implanted radiopaque markers. *Int J Radiat Oncol Biol Phys*. 2002;**52**(3):699-

703.

18. Pouliot J, Aubin M, Langen KM, Liu YM, Pickett B, Shinohara K, et al. (Non)-migration of radiopaque markers used for on-line localization of the prostate with an electronic portal imaging device. *Int J Radiat Oncol Biol Phys*. 2003;**56**(3):862-6.

19. Madsen BL, Hsi RA, Pham HT, Presser J, Esagui L, Corman J, et al. Intrafractional stability of the prostate using a stereotactic radiotherapy technique. *Int J Radiat Oncol Biol Phys*. 2003;**57**(5):1285-91.

20. Chung PW, Haycocks T, Brown T, Cambridge Z, Kelly V, Alasti H, et al. On-line aSi portal imaging of implanted fiducial markers for the reduction of interfraction error during conformal radiotherapy of prostate carcinoma. *Int J Radiat Oncol Biol Phys*. 2004;**60**(1):329-34.

21. Dehnad H, Nederveen AJ, van der Heide UA, van Moorselaar RJ, Hofman P, Lagendijk JJ. Clinical feasibility study for the use of implanted gold seeds in the prostate as reliable positioning markers during megavoltage irradiation. *Radiother Oncol*. 2003;**67**(3):295-302.

22. Khan F. *The physics of radiation therapy*. ed r, editor. Philadelphia: Lippincott Williams & Wilkins; 2003.

23. Dawson LA, Litzenberg DW, Brock KK, Sanda M, Sullivan M, Sandler HM, et al. A comparison of ventilatory prostate movement in four treatment positions. *Int J Radiat Oncol Biol Phys*. 2000;**48**(2):319-23.

24. Krempien RC, Schubert K, Zierhut D, Steckner MC, Treiber M, Harms W, et al. Open low-field magnetic resonance imaging in radiation therapy treatment planning. *Int J Radiat Oncol Biol Phys*. 2002;**53**(5):1350-60.

25. Khoo VS, Padhani AR, Tanner SF, Finnigan DJ, Leach MO, Dearnaley DP. Comparison of MRI with CT for the radiotherapy planning of prostate cancer: a feasibility study. *Br J Radiol*. 1999;**72**(858):590-7.

26. Wu J, Haycocks T, Alasti H, Ottewell G, Middlemiss N, Abdolell M, et al. Positioning errors and prostate motion during conformal prostate radiotherapy using on-line isocentre set-up verification and implanted prostate markers. *Radiother Oncol*. 2001;**61**(2):127-33.

27. Padhani AR, Khoo VS, Suckling J, Husband JE, Leach MO, Dearnaley DP. Evaluating the effect of rectal distension and rectal movement on prostate gland position using cine MRI. *Int J Radiat Oncol Biol Phys*. 1999;**44**(3):525-33.

28. Boer Hd, Os Mv, PP Jansen ea. Application of the No Action Level (NAL) protocol to correct for prostate motion based on electronic portal imaging of implanted markers. *Int J Radiat Oncol Biol Phys*. 2005;**61**:969–83.